J Polym Environ (2011) 19:546–558
DOI 10.1007/s10924-011-0282-8

ORIGINAL PAPER

Poly(vinyl alcohol-co-lactic acid)/Hydroxyapatite Composites: Synthesis and Characterization

Nita Tudorachi · Aurica P. Chiriac

Abstract There is a wide range of applications where calcium phosphate and hydroxyapatite (HA) are used as biomaterials, e.g. as synthetic bone grafts, coating on metal prostheses (like hip endoprostheses or dental implants) and drug carriers. In the study, the design and synthesis of composites based on poly(vinyl alcohol-co-lactic acid)/hydroxyapatite (PVA-co-LA/HA) with potential for biomedical applications, they are presented. The hydroxyapatite particles were surface-grafted with L(+)-lactic acid in the presence of manganese acetate as catalyst, resulting in modified hydroxyapatite (HA_m) with improved capacity of bonding, respectively for the preparation of the composite based on PVA-co-LA/HA_m. FT-IR spectra further confirmed the existence of PLA polymer on the surface of HA particles. In synthesis of PVA-co-LA copolymer the different molar ratios PVA/LA (2/1, 1/1, 1/2), toluene/water: 1/2 (as azeotrope solvent mixture) and manganese acetate as catalyst, were used. The composite materials were synthesized in situ with 10 wt% HA, and respectively HA_m (reported to PVA and lactic acid components). The composite materials were characterized by FTIR spectroscopy, thermal analyses (DSC, DTG), ^{1}H-NMR spectroscopy, particle size distribution and zeta potential.

Keywords Biomaterials · Copolymers · Poly(vinyl alcohol-co-lactic acid)/hydroxyapatite · Composites

N. Tudorachi · A. P. Chiriac (✉)
“Petru Poni” Institute of Macromolecular Chemistry,
700487 Iasi, Romania
e-mail: achiriac1@yahoo.com

Introduction

Biomaterials are materials of natural or man-made origin that are used to direct, supplement, or replace the functions of living tissues of the human body [1–3]. Biomaterials in the form of implants and medical devices are widely used to replace and/or restore the function of traumatized or degenerated tissues or organs, to assist in healing, to improve functions, to correct abnormalities and thus improve the quality of life of the patients. Hydroxyapatite (HA) is the major inorganic constituent of natural bone [4]. Hydroxyapatite has been used as implant material owing to its ability to form strong bonds with the human hard tissue. However, the pure HA is suitable only for the repair of non-load-bearing bones because of its fragility, low mechanical strength, easy rupture and weak fatigue resistance; it can not withstand the normal operating loads of bone or joints [5]. On the other hand, alumina (α-Al_2O_3) has high wear resistance, high strength and very stable chemical properties in the physiological environment. But alumina forms no chemical or biological bond at the material-tissue interface. Thus, HA coatings on the surface of alumina substrates can be used to combine the excellent bioactivity of HA with the superior mechanical properties of the substrates [6]. The composites of HA particles with biodegradable polymers have attracted much attention owing to their good osteoconductive properties. Thus, hydroxyapatite was combined with a number of natural or synthetic polymers, the resulting composites are expected to have better mechanical properties than neat (unreinforced) polymers as well as improved structural integrity and flexibility over brittle glasses and ceramics, for eventual load-bearing applications. PLA with large amount of L-form isomer (PLLA) is highly crystalline. Its inherent brittleness is a major disadvantage for potential industrial applications. The flexibility of PLA can be improved through copolymerization and blending processes. Blending with other biodegradable polymers allows the modifying the properties of hard and brittle PLLA. Several blend systems containing PLLA have been investigated, such as PLLA/poly(ethylene glicol) (PLLA/PEG) [7–9], PLLA/poly(3-hydroxybutyrate) (PLLA/PHB) [10] and PLLA/poly(ε-caprolactone) (PLLA/PCL) [11, 12]. However, there is evidence that these blends are not stable and their attractive mechanical properties are lost over time.

At the beginning of 1980s, as one of the most promising high performance bone repair and replacement materials were HA/PLA composites, and during the last years, investigations on preparation, mechanical properties, interface structure, biocompatibility and biodegradability of the composites have became more active [13–15]. The results of those studies showed that HA particles were in lack of adhesion with the polymer matrix. The improvement of the interfacial adhesion between the HA particles and polymer matrices has become the key technique in preparing the composites. In this order, various methods have been purposed to modify the surface of HA particles, such as agents coupling as for example silane [16], dodecyl alcohol [17], polyacids [18–20], polyethylene glycol [21], and isocyanate [22–24]. In all these techniques, the coupling agents were reacted with the hydroxyl groups on the surface of HA particles and thus the affinity of particle surface to the polymer matrix was improved to some extent. In recent years, emphasis in biomaterial engineering has moved from materials that remain stable in the biological environment to materials that can degrade in the body. Biodegradable materials are designed to degrade gradually and be replaced eventually by newly formed tissue in the body. Biodegradable polymers such as poly(ε-caprolactone) (PCL), copoly-L-lactide (CPLA) [25], poly(glycolic acid) (PGA) [26] and their copolymers, poly (D,L-lactic-co-glycolic acid) (PLGA) are known for their variable degradation characteristics, as well as reasonable mechanical properties [25–29].

Poly(vinyl alcohol) (PVA) is recognized as one of the very few vinyl polymers soluble in water also susceptible of ultimate biodegradation in the presence of suitably acclimated microorganisms. Accordingly, increasing attention is devoted to the preparation of environmentally compatible PVA-based materials for a wide range of applications [30]. PVA's rheological properties, particularly its ability to produce highly resistant films and its hydrophilic character, account for the improvements in the mechanical properties and performances of natural polymers when mixed with PVA. Accordingly, several investigations were carried out on the rheological and structural characterization of materials obtained by mixing PVA, either in solution or in the melt, with several natural polymers of vegetal, animal, and marine origin, such as cellulose, lignin, starch, silk, gelatin, chitin, and chitosan [31]. The inherent hydrophilicity of poly(vinyl alcohol) (PVA) makes it an attractive polymer for applications based on membranes. Its thermal and chemical resistance and a high anti-fouling potential are accompanied by high water permeability. The large swelling capacity requires that the PVA be adequately linked into a matrix to ensure that its properties are able to formulate. Also, the alcohol-substituted polymers, however, show higher melting temperature and a weaker property dependence on comonomer content [32].

A composite material containing both a bioceramic and a biodegradable polymer could offer the necessary benefits in terms of exhibiting both osteogenic characteristic of ceramic material and biodegradable property of the polymer and could also offer improved mechanical properties.

The literature in the field mention about the possibilities for modifying the hydroxyapatite particles by directly grafted of poly(lactic acid) onto the hydroxyl group of the surface of hydroxyapatite particles by ring-opening polymerization of L-lactide in xylene and in the presence of stannous octanoate ($Sn(Oct)_2$) as catalyst process followed by grafted compound incorporation into poly(lactic acid) to form the composite [33–35].

The objective of this research is to synthesize composites based on poly(vinyl alcohol-co-lactic acid)/hydroxyapatite (PVA-co-LA/HA) with potential biomedical applications. The modification of the HA surface was performed to obtain a composite with improved binding capacity between the constitutive compounds, respectively HA and the polymeric matrix based on PVA-co-LA, biodegradable and biocompatible polymeric compounds with extended applications in medical and pharmaceutical field. The hydroxyapatite particles were surface-grafted with L(+)-lactic acid (90 wt% aqueous solution) in the presence of manganese acetate as catalyst, resulting in modified hydroxyapatite (HA_m) with improved capacity of bonding, respectively for the preparation of the composite based on PVA-co-LA/HA_m.

Two composite materials, based on 10 wt% HA or HA_m respectively, with different molar ratios between PVA and LA of about 2/1, 1/1, and 1/2, using the toluene/water mixture (1/2) as azeotrope solvent and manganese acetate as catalyst, they were synthesized in situ. Based on the preparation conditions and the ratio between the compounds (reported to compounds weight), the composite materials were noted PVA-co-LA/HA (2/1/10; 1/1/10; 1/2/10) and PVA-co-LA/HA_m (2/1/10; 1/1/10; 1/2/10), respectively.

Experimental

Materials

The raw materials used in our experiments were available as commercial products and were analytical grade reagents. Poly(vinyl alcohol) (PVA), hydrolysis degree 98%, degree of polymerization DP = 400, saponification index 140 ± 30 mg KOH/g from Romacryl S.A. (Romania). L(+)-lactic acid [(S)-2-hydroxypropionic acid] (LA) aqueous solution 90 wt% from Fluka (Switzerland) was used without further purification. Hydroxyapatite [$Ca_{10}(PO_4)_6(OH)_2$] from Fluka (Switzerland) and modified hydroxyapatite with L(+)-lactic acid (HA_m) were utilized as fillers in composite materials. Manganese acetate [$(CH_3COO)_2Mn\cdot4H_2O$], toluene, tetrahydrofuran, acetone were analytical grade reagents from Chimopar S.A. (Romania) and were used as received.

Modification of Hydroxyapatite Surface

The modification of HA surface was achieved by a condensation reaction with LA. Initially, carboxyl groups of LA react with hydroxyapatite and a calcium carboxylate linkage is obtained by water removal [20]. A typical procedure for HA surface grafting is briefly described, as follows: firstly, 20 g HA was dispersed in tetrahydrofuran (150 mL), under stirring at room temperature for 30 min. Then, 20 g LA in which were introduced 0.1 g manganese acetate as catalyst (0.5 wt% reported to LA) were slowly dropped into the above stirred suspension. The molar ratio LA/HA was 11/1. The suspension was heated to 60–70 °C with reflux and maintained for 60 min, then about 80 mL tetrahydrofuran was removed. Then 80 mL toluene (to form an azeotrope with water—at a ratio of 1–2 toluene/water) were added into the reaction mixture, afterwards the mixture was heated and maintained at 120–130 °C for 6 h. After cooling at room temperature, the reaction mixture was washed several times with tetrahydrofuran to remove PLA homopolymer, and then it was isolated by centrifugation (5,000 rot/min). The solid reaction product was again suspended in tetrahydrofuran; next it was stirred for 30 min and separated by centrifugation. Then, it was again dispersed under stirring in acetone for 3–4 h to remove the PLA homopolymer not grafted on hydroxyapatite particles surface, and finally it was isolated by centrifugation and was dried under vacuum 24 h at 60–70 °C. Also, the reaction products were several times washed with tetrahydrofuran and acetone as well as centrifuged for the completely remove of the toluene traces. The absence of toluene traces in the structure of the prepared composites is confirmed by IR spectra: they are missing the specific triade peaks of toluene from 1,803, 1,858, 1,942 cm^{-1} as well as the correspondingly aromatic C=C stretches peak around of 1,475 cm^{-1} [36, 37]. The reaction yield of hydroxyapatite modification with L(+)-lactic acid was approximately 58%.

Scheme 1 illustrates a possible reaction mechanism for hydroxyapatite modification.

Composites Preparation

In order to improve the bonding between HA particles and polymer matrix the HA particles were surface—grafted with PLA and further used in situ composites synthesis. This stage, HA_m and HA were utilized to obtain PVA-co-LA/HA_m and PVA-co-LA/HA composite materials. The composite materials with 10 wt% HA or HA_m and the different molar ratio PVA/LA (2/1, 1/1, 1/2), were achieved. The reaction was developed by a solution polycondensation mechanism using toluene/water (1/2) as azeotrope solvent mixture and manganese acetate as catalyst (0.8 wt% reported to PVA and LA). Poly(vinyl alcohol), in previously established quantities was dissolved under stirring in water at 70 °C (15–18 wt% concentration solutions), and adequate quantities of LA and manganese acetate aqueous solutions were added drop by drop. After homogenization of the reaction components for 30 min, HA or HA_m (10 wt% reported to PVA and LA) were added and the reaction in two-step was achieved. In the first step the reaction took place under reflux at 95 °C for 3 h and in the second step, the adequate quantity of toluene was carefully added by dropping and reaction developed 3 h at 115–120 °C. Water and by-products obtained were removed by azeotropic dehydration using toluene. The reaction product was then maintained for 15 min at 130–135 °C and then cooled at 50–60 °C and poured in a Petri dish. Composites drying was done at 70–80 °C under vacuum during 48 h. The PLA homopolymer grafted on

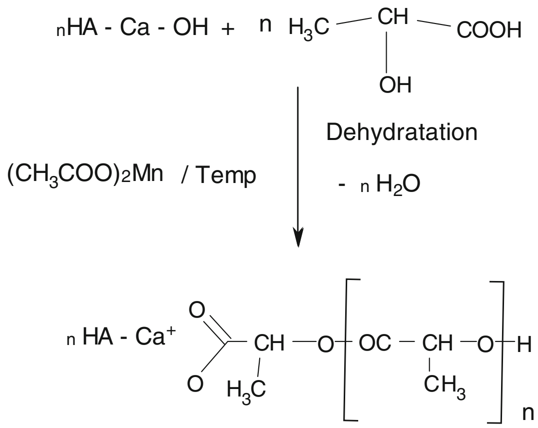

Scheme 1 Idealized reaction mechanism of HA modification with L(+)-lactic acid

the HA surfaces, as inter-tying molecules, plays an important role in improving the cohesion strength between particles and the polymer matrix and the PVA-co-LA/HA$_m$ composites exhibit higher characteristics than PVA-co-LA/HA.

Characterization

FTIR spectra were recorded using a spectrophotometer Vertex 70 model (Germany). The samples were homogenized and pressed on KBr pellets.

^{1}H-NMR spectra of the copolymers were obtained on a Bruker Avance DRX 400 NMR spectrophotometer (Germany), equipped with 9.4 Tesla ultrashield magnet (400 MHz). The samples were dissolved in D_2O with a concentration of about 5 wt%. The analysis was carried out at 25 °C and chemical shifts were reported in parts per million (ppm) using tetramethylsilane (TMS) as the internal reference.

Measurement of particle size was done with a Mastersizer 2000 system (version 5.31) Malvern Instruments (England). The system is constituted of an optical bank which uses a laser light He–Ne of 632 nm and 2 mW power, a sample dispersion unity Hydro 2000A type equipped with stirrer, recirculating pump and ultrasonic source. The measurement domain is between 0.020 and 2,000 μm.

Zeta potential and *conductivity* were measured using a Zetasizer Nano-ZS, ZEN-3500 model, Malvern Instruments (England). Also, hydrodynamic diameter and polydispersity were determined using noninvasive backscatter (NIBS) technology, which allows sample measurement in the range of 0.6 nm–6 μm. For measurement, the copolymers were dissolved in twice distilled water at a concentration of 1 g/L. The measurement was carried out using a laser green light He–Ne (532 nm) as light source at a fixed angle of 173°. The following parameters were used for experiments: water as dispersant medium with refractive index 1.330, viscosity 0.887 cP, dielectric constant 79 and 25 °C temperature. After size measurement, zeta potential was measured with the M3-PALS technique which is a combination of Laser Doppler Velocimetry (LDV) and Phase Analysis Light Scattering (PALS). Electrophoretic mobilities of particles were measured and converted to zeta potential using Henry Equation:

$$U_E = \frac{2\varepsilon Z f(ka)}{3\eta} \tag{1}$$

where U_E—electrophoretic mobility, ε—dielectric constant of the medium, Z—zeta potential, η—viscosity, f(ka)—Henry function (for aqueous medium $f(ka) = 1.5$ and refer to Smoluchowski constant). Also, conductivity is measured simultaneously with zeta potential. The average of five measurements is presented as value for zeta potential and conductivity.

The thermogravimetric analyses of composite materials were performed using a thermogravimetric balance STA 449F1 Jupiter model (Netzsch—Germany). Samples with a mass ranging from 7 to 10 mg were heated from 30 to 600 °C, with heating rates of 5, 10 and 20 °C/min. Nitrogen gas (99.99% purity) as carrier with flow rate of 50 mL/min and protective purge for thermobalance of 20 mL/min was used. The samples were heated in open Al_2O_3 crucible, and Al_2O_3 as reference material was used. The temperature calibration of the thermobalance was made according to the procedure reported in the user's manual of the equipment. Thermal decomposition of composite materials with 10% HA or HA$_m$ in which the PVA/LA molar ratio is 1/1 was performed at three different heating rates (5, 10, 20 °C/min), in nitrogen atmosphere.

DSC thermal analyses were carried out by means of a differential scanning calorimeter Perkin Elmer Pyris Diamond with a heating rate of 10 °C/min in nitrogen atmosphere. The first heating run was carried out with 10–12 mg sample in the temperature range between room temperature and 250 °C. The second heat was recorded with same sample that was rapidly cooled at room temperature and heated to 200 °C approximately. Pure indium was used as standard for calorimetric calibration.

Results and Discussion

FTIR and ^{1}HNMR Characterization

FTIR spectra of HA and HA$_m$ are presented in Fig. 1 and agree well with the literature in the field [38, 39]. In the HA spectrum the presence of some absorption bands at 3,437 and 3,571 cm^{-1} are attributed to νOH stretching vibrations, and at 1,639 cm^{-1} due to adsorbed water at the surface of HA particles. Also, stretching vibrations of phosphate anion (νPO_4^{3-}) are remarked at 962, 1,031 and 1,090 cm^{-1} and the deformation vibrations (δPO_4^{3-}) are present at lower frequencies 564 and 601 cm^{-1}. In the case of the grafted HA with LA, except the HA characteristic absorption bands, some additional vibration bands appear evidencing the reaction of the carboxylic groups of LA with the hydroxyl groups from HA surface (in this case ester linkages are obtained) or with Ca^{2+} ions when calcium carboxylate is obtained. So, it can be remarked the presence of a pronounced absorption band at 1,756 cm^{-1} belonging to stretching vibrations ($\nu C = O$) of the ester group obtained in the reaction and of some absorption bands at 1,370–1,426 cm^{-1} belonging to calcium carboxylate (stretching vibrations νCOO^-). Other bands, not registered in case of unmodified HA, must also be

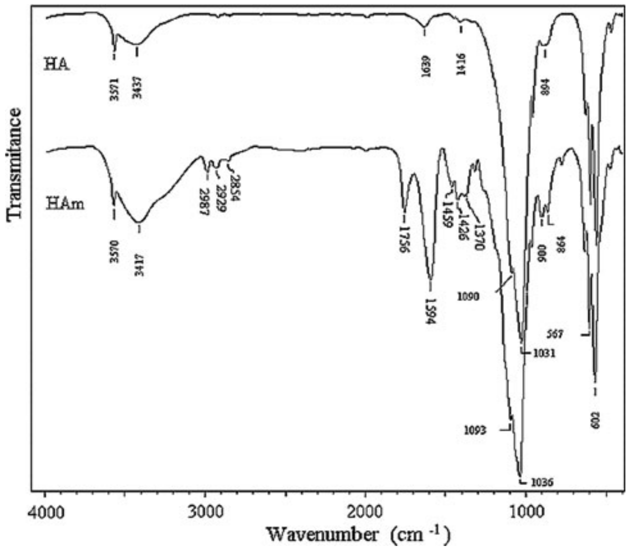

Fig. 1 FTIR spectra of HA and HA_m

evidenced, bands that belong to CH and CH_3 groups from lactic acid. Thus, the vibrations of methine groups (νCH) at 2,854 $cm^{-1}$and the stretching vibrations of methyl groups (νCH_3) from 2,929 to 2,987 cm^{-1} must be noticed. As HA particles were intensely washed after the grafting reaction with tetrahydrofuran and acetone (good solvents for PLA), the possibility that IR peaks belonged to the homopolymer physically adsorbed, it was excluded. All these additional bands noticed in HA_m spectrum support its modification with lactic acid by chemical linkages.

FTIR spectrum of PVA-co-LA/HA_m composite (Fig. 2) display characteristic absorption bands of HA_m, at 1,044 and 1,131 cm^{-1} bands corresponding to the stretching vibrations $\nu PO_4{}^{3-}$ of the anion phosphate and also at 558, 650 cm^{-1} corresponding to bending vibrations $\delta PO_4{}^{3-}$. The absorption band of 1,377 cm^{-1} attributed to calcium carboxylate acquired in the reaction of Ca^{2+} ions with carboxylic group (stretching vibrations νCOO^-) is noticed in the composite material. Also, a pronounced absorption band at 1,744 cm^{-1} belonging to the ester groups (νC=O) and another one at 3,432 cm^{-1} corresponding to stretching vibrations νOH of the PVA chains are also registered.

^{1}H-NMR spectrum of PVA-co-LA copolymer is presented in Fig. 3. Based on the reports of peak assignments for proton species in PVA and PVA derivatives [40, 41], were assigned the proton signals in the ^{1}H-NMR spectrum of PVA-co-LA copolymer, as given in Fig. 3. The resonance at $\delta = 1.299$ ppm is attributed to the sequences of lactic acid units CH_3 (d) grafted to PVA chain. The signal appearing at 1.415 ppm is assigned to methylene groups CH_2 (a) existent in PVA backbone structure, the signal at 3.651 ppm is attributed to methine protons CH (c) in lactic acid structure and the signal at 4.793 ppm to methine protons CH (b) in PVA backbone structure of the copolymer. Residual proton signal of D_2O appeared at 4.238 ppm.

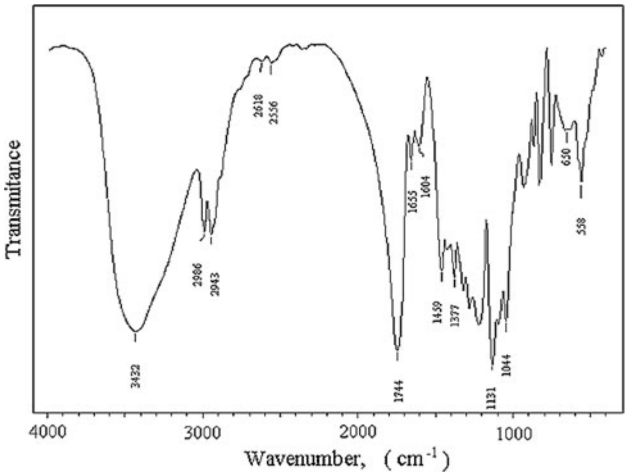

Fig. 2 FTIR spectrum of PVA-co-LA/HA_m composite

As it is well known, two clearly distinct peaks appear in the ^{1}H-NMR spectrum of lactic acid—at 1.41 ppm of the methyl group and at 4.38 ppm for the methine C–H bond—and each peak corresponds to a different chemical environment for hydrogen in this molecule.

The chemical shifts of the mentioned peaks from 1.41 to 1.299 are attributed to the additional magnetic field intervened from methylene groups of PVA as well as owing to the solvent signal from 4.238 ppm in case of the second peak.

Thermal Characterization

The TG and DTG curves of thermal decomposition of HA, HA_m, PVA-co-LA/HA and PVA-co-LA/HA_m composites, in Figs. 4, 5, 6 are presented within the 30–600 °C temperature range. The most important thermogravimetric characteristics are temperature at which the thermal decomposition begins (T_{onset-}), the temperature at which the degradation rate is maximum (T_{peak-}), the temperature at ending process ($T_{endset-}$) and the mass losses in each stage ($W_{\%}$)—and they are presented in Table 1.

The amount of lactic acid grafted on HA surface was determined from data recorded by thermogravimetric analysis. The total mass loss from HA (W_{HA}) and HA_m (W_{HAm}), recorded at 600 °C, were about 3.20 and 18.60%, respectively. As it is well known HA as hydrated calcium phosphate material begins to dehydroxylate around of 800 °C to form oxyhydroxyapatite through a gradual process which takes place over a range of temperatures. From the registered thermogravimetric data up to 600 °C it was established the lactic acid mass [$M_{(L-LA)}$] grafted on HA surface which was calculated by the following relationship:

Fig. 3 ^{1}H-NMR spectrum of PVA-co-LA copolymer

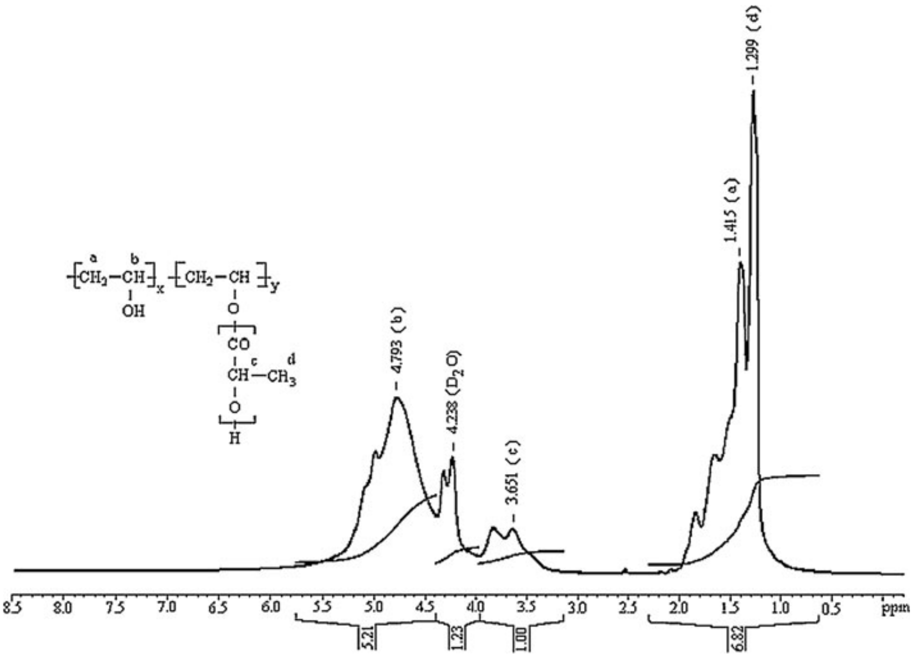

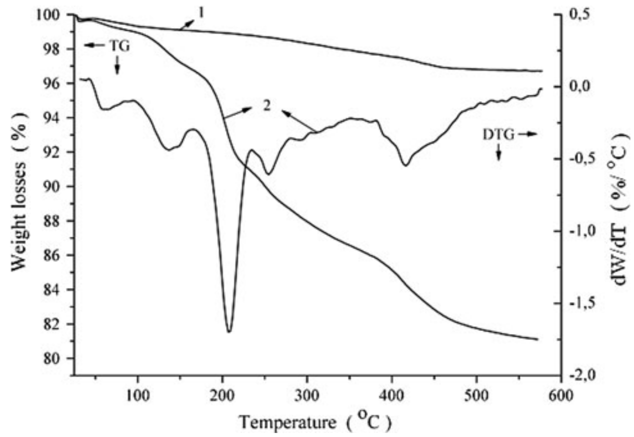

Fig. 4 TG and DTG curves recorded at thermal decomposition of HA and HA$_m$

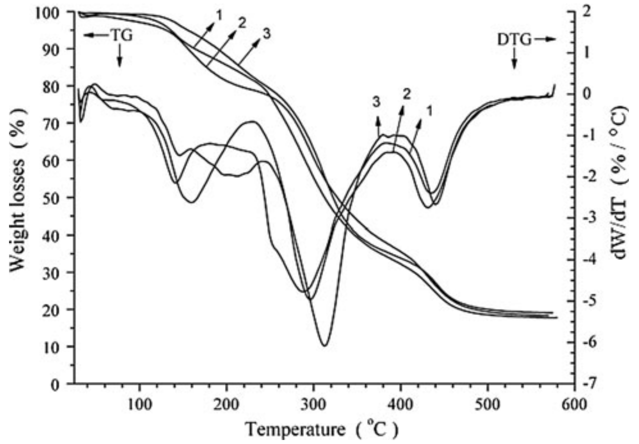

Fig. 5 TG and DTG curves recorded at thermal decomposition of PVA-co-LA/HA composites [1- PVA-co-LA/HA(1/1/10); 2-PVA-co-LA/HA (2/1/10); 3-PVA-co-LA/HA (1/2/10)]

$$M_{(L-LA)} = W_{HAm} - W_{HA} = 18.60 - 3.20\,\% = 15.40\,\% \tag{2}$$

At the same time the thermal behavior of the prepared composites is influenced by products composition, respectively the hydroxyapatite type (HA or HA$_m$) and PVA/LA molar ratio used in the initial mixture of copolymers synthesis. Thus, the thermal stability of the two types of composite materials decreases with the increase of the lactic acid content into the copolymers structure and raises in case of composite with grafted hydroxyapatite (HA$_m$). Accordingly, PVA-co-LA/HA (2/1/10) composites recorded mass loss of 50% at 329 °C and PVA-co-LA/HA (1/2/10) at 319 °C. On the other hand, PVA-co-LA/HA$_m$ (2/1/10) recorded 50% weight loss at 365 °C and PVA-co-LA/HA$_m$ (1/2/10) at 330 °C. Generally, based on the TG and DTG registered graphs, the study indicates the presence of 3–4 stages of thermal decomposition for each composite material where mass losses occur with different rates.

The kinetics of thermally stimulated reactions of composite materials can be described by the basic Eq. 3 [42].

$$\frac{d\alpha}{dt} = k \cdot f(\alpha) \tag{3}$$

where α is the conversion degree ($\alpha = (W_0 - W_t)/(W_0 - W_f)$, W_t, W_0, and W_f are weights at initial, time t and final time of the sample, respectively), $d\alpha/dt$ is the conversion rate, $f(\alpha)$ is the differential expression of a kinetic model function which depends on the particular

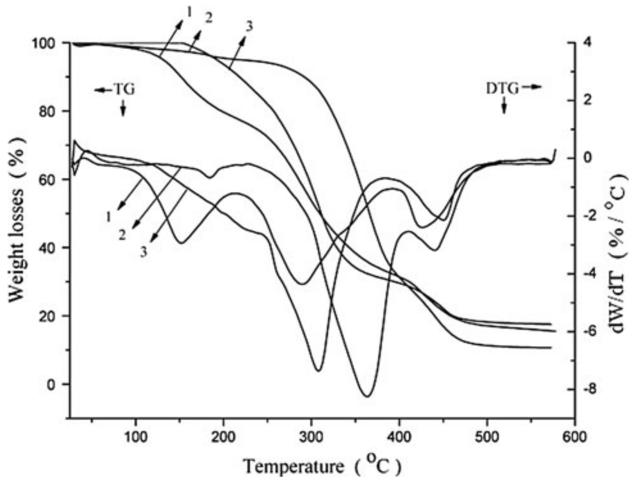

Fig. 6 TG and DTG curves recorded at thermal decomposition of PVA-co-LA/HA$_m$.composites [1- PVA-co-LA/HAm (1/1/10); 2-PVA-co-LA/HAm (2/1/10); 3-PVA-co-LA/HAm (1/2/10)]

degradation mechanism and k is the Arrhenius rate constant, which is given as Eq. 4:

$$k = A\exp\left(-\frac{E}{RT}\right) \tag{4}$$

where A is the pre-exponential factor (s^{-1}), assumed to be independent of temperature, E is the activation energy of decomposition reaction ($kJmol^{-1}$), T is the absolute temperature (K), and R is the gas constant (8.314 $Jmol^{-1}$ K^{-1}). Substituting "k" from Eq. (4) into Eq. (3) it obtains:

$$\frac{d\alpha}{dt} = A\exp\left(-\frac{E}{RT}\right)\cdot f(\alpha) \tag{5}$$

For non-isothermal measurements at constant heating rate $\beta = dT/dt$, and $f(\alpha) = n(1-\alpha)$ for one-step reactions type Fn, Eq. (5) transforms to:

$$\frac{d\alpha}{dT} = \frac{A}{\beta}\exp\left(-\frac{E}{RT}\right)\cdot n(1-\alpha) \tag{6}$$

or:

$$\ln\left(\frac{d\alpha}{dT}\right) = \ln\left(\frac{A}{\beta}\right) + n\cdot\ln(1-\alpha) - \frac{E}{RT} \tag{7}$$

Eqs. (5) and (7) are the fundamental expressions of analytical methods to calculate kinetic parameters on the basis of TG data in isothermal and non-isothermal measurement, respectively [43, 44]. The kinetic parameters were obtained using NETZSCH Thermokinetics software as Multiple-linear Regression (MLR) [45].

The determined values of the kinetic parameters (E, n, and log A) are presented in Table 2. For the same PVA/LA molar ratios and in similar thermal decomposition conditions, kinetic parameters are different, being influenced by hydroxyapatite type (HA or HA$_m$). In the case of composites with HA$_m$, activation energy (E) is higher and implies existence of better cohesion between inorganic material and copolymer. Weight losses (W) shown in table are recorded at the end of thermal decomposition process (600 °C) and depend on heating rate.

The variation of activation energy and pre-exponential factor log A, depending on the conversion degree of thermal decomposition reactions, it is presented in Figs. 7 and 8. The variations of these parameters are similar for both composites. Initially, the two kinetic parameters values are slightly decreased after which the recorded values increase. Two peaks appear around the conversion degrees of 0.25 and 0.70 conversion (PVA-co-LA/HA), and respectively 0.30 and 0.80 (PVA-co-LA/HA$_m$). A significant drop parameters that occur at 0.8–0.9 conversion corresponds to the 300–400 °C temperature domain undergoing significant weight losses. The kinetic parameters variation related on the thermal decomposition conversion designates complex mechanisms of thermal degradation corresponding to the constituent components that take place at several stages with different ratios and sometimes with overlapping processes.

In Table 3 and Figs. 9, 10 the thermal characteristics of composite materials PVA-co-LA/HA$_m$ and PVA-co-LA/HA determined by differential scanning calorimetry (DSC), are presented. It was ascertained that PVA-co-LA/HA$_m$ composite materials present only one T_g value (glass transition temperature), and the melting temperatures (T_m) of these composites are in the range of 170–195 °C and vary with PVA/LA molar ratio in their structure. On the other hand, the PVA-co-LA/HA composite materials present two T_g values, demonstrating that there is not a good compatibility between components and phase separations can occur. The melting temperatures of PVA-co-LA/HA composite materials are situated around 140 °C (Fig. 8). These findings demonstrate that the lactic acid grafted on the HA surface can also participate to some condensation reactions that take place during the composite materials synthesis, forming new chemical linkages. So, hydroxyapatite modified with lactic acid can contribute to compatibility improvement of the components in the composite structure. The hydroxyapatite particles distribution is also more uniform and homogeneous promoting better thermal properties.

The literature data [46] mention that during poly(lactic acid) decomposition two distinct peaks appear: the first peak at 295 °C attributed to the depolymerization and exclusively formation of lactide. The second peak at 350 °C is due to other decomposition processes the main products being carbon oxides, acetaldehyde, lactide and further cyclic oligomers up to nine monomer units.

Thermal degradation of PVA has been also extensively reported in literature [47]. An endothermic peak at 60–90 °C, was attributed to the loss of moisture.

Table 1 Thermal characteristics of HA, HA_m and composite materials

Sample	Molar ratio PVA/LA	Degradation step	T_{onset} (°C)	T_{peak} (°C)	T_{endset} (°C)	W (%)	T_{50} (°C)
HA	–	I	390	570	580	3.20	–
		residue				*96.80*	
HA_m	–	I	103	137	161	2.78	–
		II	186	208	226	5.57	
		III	246	254	275	2.44	
		IV	395	416	446	7.82	
		residue				*81.39*	
PVA-co-LA/HA	2/1	I	127	161	214	21.11	329
		II	258	298	335	41.92	
		III	409	434	574	18.47	
		residue				*18.50*	
	1/1	I	110	141	163	14.76	310
		II	237	287	338	51.97	
		III	409	435	473	14.94	
		residue				*18.33*	
	1/2	I	115	143	154	5.94	319
		II	187	209	233	13.90	
		III	258	309	344	44.50	
		IV	411	437	470	16.40	
		residue				*19.26*	
PVA-co-LA/HA_m	2/1	I	165	185	196	5.00	367
		II	288	364	394	67.20	
		III	414	450	481	18.48	
		residue				*9.32*	
	1/1	I	112	151	201	22.42	318
		II	237	289	347	45.15	
		III	406	426	481	16.60	
		residue				*15.83*	
	1/2	I	120	–	231	17.32	330
		II	247	308	339	52.00	
		III	408	450	470	13.20	
		residue				*17.48*	

Italics indicates the amount of inert residue remaining after the thermal decomposition

Table 2 Kinetic parameters of composite materials with HA or HA_m

Sample	Molar ratio PVA/LA/HA (mol/mol/%wt.)	E_a (kJ/mol)	Log A ($s^{-1)}$	n	β (°C/min)	W (%)
PVA-co-LA/HA	1/1/10	62.24	3.462	2.73	5	84.97
					10	81.60
					20	79.98
PVA-co-LA-/HA_m	1/1/10	69.43	2.249	2.52	5	85.60
					10	84.20
					20	82.50

Also, PVA displayed a major endothermic peak at about 230 °C, which is attributed to its melting. Three steps of weight loss, located at about 100, 200, and 300 °C are attributable to a loss of moisture, while those at higher temperature are related to processes involving both melting of PVA chains and the onset of degradation. Another drop at above 300 °C is indicative of the occurrence of more extensive thermal degradation processes.

These data support the affirmation about the overlapping processes of degradation corresponding to the constituent

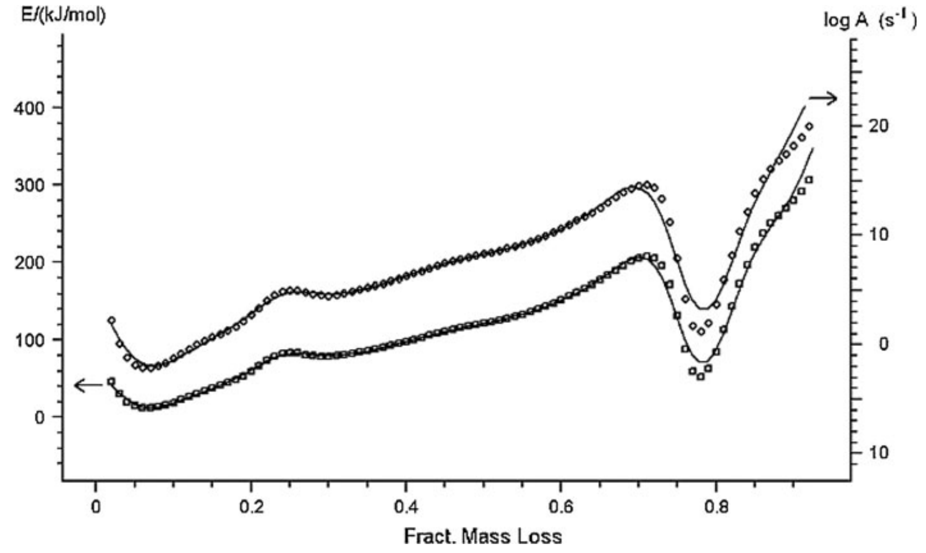

Fig. 7 Variation E_a and log A with thermal decomposition conversion of PVA-co-LA/HA (1/1/10) composites

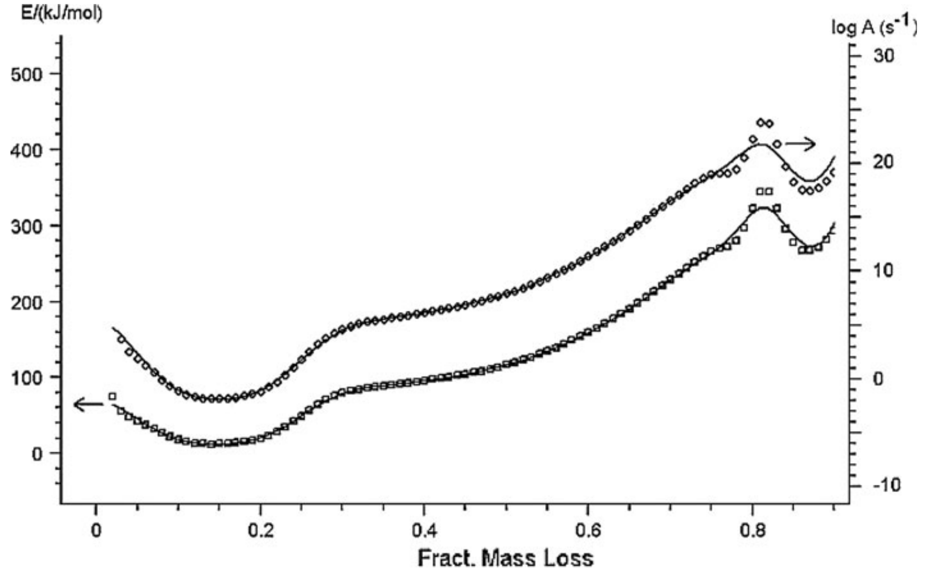

Fig. 8 Variation E_a and log A with thermal decomposition conversion of PVA-co-LA/HA_m (1/1/10) composites

Table 3 Thermal characteristics determined by DSC

Sample	PVA/LA/HA (mol/mol/wt%)	T_{g1} (°C)	T_{g2} (°C)	T_m (°C)
PVA-co-LA/HA_m	2/1/10	41	–	195
	1/1/10	37	–	170
	1/2/10	19	–	185
PVA-co-LA/HA	2/1/10	11	67	141
	1/1/10	10	66	143
	1/2/10	−3	58	139

components as well as the exhibiting of the two glass transition points, one for each of the block copolymer partners.

Particle size Distribution

Analysis of particle size distribution by laser diffraction method with Mastersizer-2000 equipment of HA, HA_m, PVA-co-LA/HA_m (1/1/10 wt%) and PVA-co-LA/HA (1/1/10 wt%) are presented in Fig. 11 and Table 4. Generally, the HA and HA_m particles diameter have a lower value than composite materials particles. Ninety wt% of the total particles volume present a diameter lower than 29.77 μm (HA) and 49.12 μm (HA_m), while in the case of composite materials, the diameter value is lower than 651.08 μm

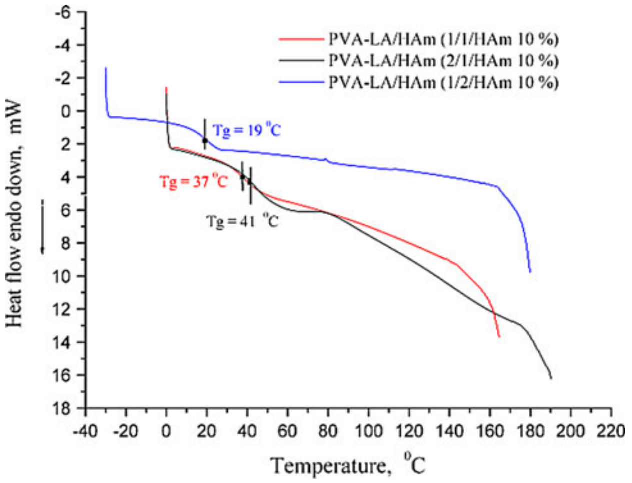

Fig. 9 DSC curves of PVA-co-LA/HA composites

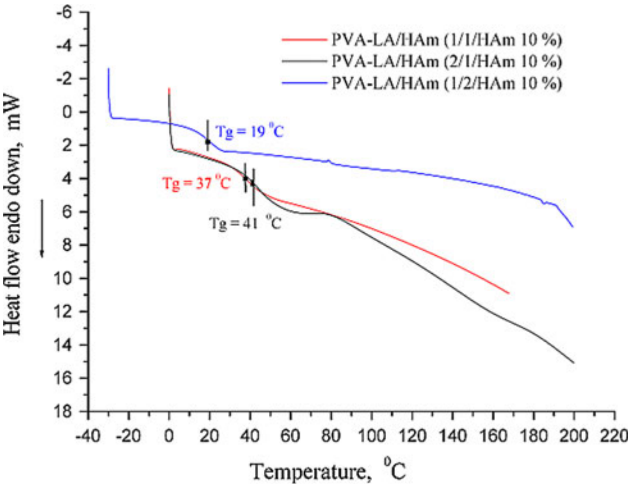

Fig. 10 DSC curves of PVA-co-LA/HA$_m$ composites

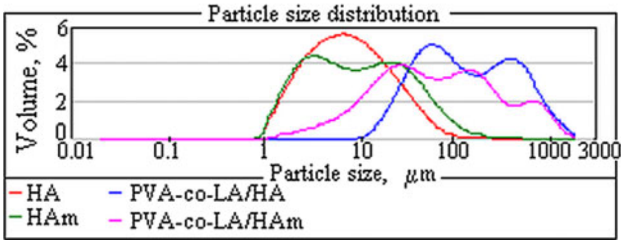

Fig. 11 Particle size distribution

(PVA-co-LA/HA), and 538.65 µm (PVA-co-LA/HA$_m$) respectively. In the case of the composites the particles size are raised due to the intermolecular associations that can occur between HA and the polymer matrix, thus leading to particles aggregation. HA particles present a more reduced polydispersity than HA$_m$, the absolute deviation from the median value of particles diameter is 1.20 (HA), compared with 1.68 (HA$_m$). In the case of the composite materials polydispersity is higher than the organic material used: PVA-co-LA/HA (1.54) and PVA-co-LA/HA$_m$ (2.40). The introduction of two types of hydroxyapatite in composite materials structure influenced in a different way the particles size. Although, HA$_m$ particles were bigger than HA ones, the composites with HA$_m$ had a decreased diameter of the particles. This fact was due to lactic acid grafted on the HA particles surface that raised the compatibility degree, improved the contact between hydroxyapatite and the polymer and yielded a more homogeneous and uniform distribution of the components in the composite material structure.

Zeta potential and Conductivity

The hydrodynamic diameter values (Z-average) and the zeta potential of the composite materials and the copolymers based on the dynamic diffusion method of laser light, were determined at 25 °C (Table 5). Zeta potential refers to electrostatic potential generated by ions accumulation at the surface of the particle (or colloid) organized in a double electric layer built up of Stern layer and a diffusion layer. The composite materials with HA$_m$ have hydrodynamic diameter bigger than the composite materials with HA, but lower than the copolymers. Also, zeta potential of composite materials with HA$_m$ present absolute intermediary values comprised between those of the copolymers and of composite materials with HA. All the nanoparticles were negatively charged in acid aqueous solution (pH 3.5–3.9), which could be possible attributed to the presence of ionized end carboxyl groups in PLA homopolymer. Zeta potential don't present high negative absolute values, as the presence of uncapped free carboxylic groups is very reduced as these groups participated at condensation reactions with OH groups of PVA and with Ca ions (Scheme 1), and the protons from the dispersion medium where the measurements were done (pH acid) neutralize most of the ions with negative charge.

Zeta potential and the electrical conductivity were studied as temperature function on 25–40 °C interval and these parameters variations are presented in Figs. 12, 13, 14, 15. The pH-values of the analyzed solutions are presented in Table 5. Generally, it is known that zeta potential of stable colloidal solutions has values situated outside the ± 30 mV domain. Since the copolymer dispersions achieved have lower absolute values of zeta potential than those earlier mentioned, they doesn't present time stability and the tendency of sedimentation is possible. At the same time, data concerning zeta potential as well as of the electrical conductivity confirm a higher stability of the composite materials performed with modified HA.

The electrical conductivity variation with temperature records a linear growth on the whole domain 25–40 °C,

Table 4 Dimensional characteristics of the hydroxyapatite and the composite materials

Sample	d(0.1) µm	d(0.5) µm	d(0.9) µm	D[3] µm	D[4] µm	Uniformity	Span
HA	2.18	7.50	29.77	5.09	12.93	1.20	3.67
HA_m	2.07	9.44	49.12	5.35	20.00	1.68	4.98
PVA-co-LA/HA (1/1/10)	32.32	128.19	651.08	78.78	256.98	1.54	4.82
PVA-co-LA/HA_m (1/1/10)	9.88	62.88	538.65	23.45	175.56	2.40	8.40

d(0.1); d(0.5); d(0.9) 10, 50, and 90% of the sample volume are particles with smaller diameter than specified in the table

D [3]—medium diameter for the equivalent sphere of the same surface with that of the particles, called also media Sauter

D [4]—medium diameter for the volume

Uniformity—is the measure of the absolute deviation from the median value. Span —represents the width of the distribution. The distribution is narrower, span value is smaller. Span value is calculated with the formula: S = [d(0.9)–d(0.1)]/d(0.5)

Table 5 Characteristics of the aqueous composite dispersions measured at 25 °C

Sample	PVA/LA/HA (mol/mol/%)	Hydrodynamic diameter		Zeta potential		Conductivity (mS/cm)
		Z-average (nm)	Polydispersity index	Z.P. (mV)	pH	
PVA-co-LA	2/1/0	246	0.536	−10.60	4.83	0.096
	1/1/0	421	0.414	−10.00	6.10	0.078
	1/2/0	345	0.451	−3.94	4.40	0.113
PVA-co-LA/HA_m	2/1/10	144	0.825	−3.09	3.59	0.991
	1/1/10	149	0.981	−3.90	3.79	1.49
	1/2/10	141	0.806	−2.34	3.79	1.33
PVA-co-LA/HA	2/1/10	95.6	0.623	−2.01	3.98	1.37
	1/1/10	53.7	1.000	−2.02	3.90	1.71
	1/2/10	60.9	0.965	−1.74	3.88	1.67

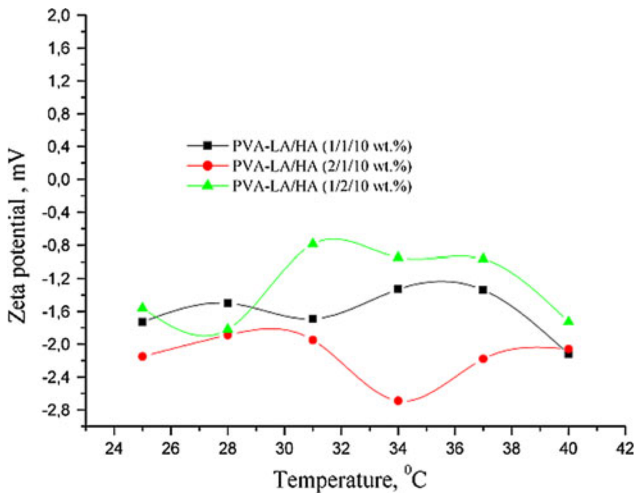

Fig. 12 Zeta potential variation with temperature for PVA-co-LA/HA composites

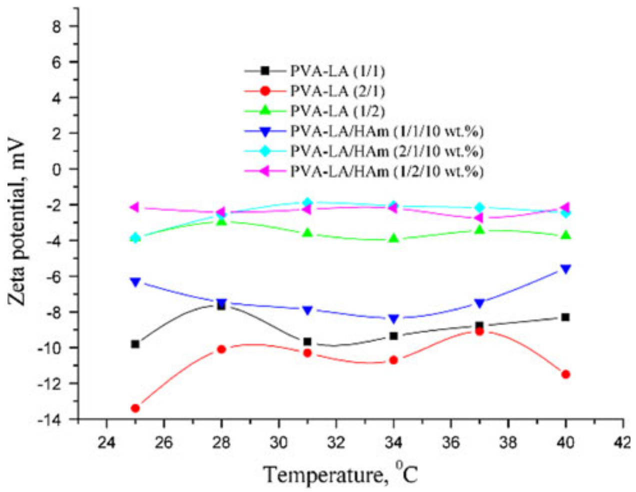

Fig. 13 Zeta potential variation with temperature for PVA-co-LA copolymers and PVA-co-LA/HA_m composites

more raised values are recorded in the case of composite materials with HA_m or HA, comparative to electrical conductivity of copolymers (Figs. 14, 15), and depend on the PVA/LA molar ratio in the structure of composite materials, respectively direct proportional with the LA content.

Conclusions

Different types of composite materials with biodegradable matrix (PVA-co-LA), different molar ratio PVA/LA (2/1, 1/1, ½) and 10 wt% HA_m or HA, were synthesized. In order to enhance bonding between HA particles and the

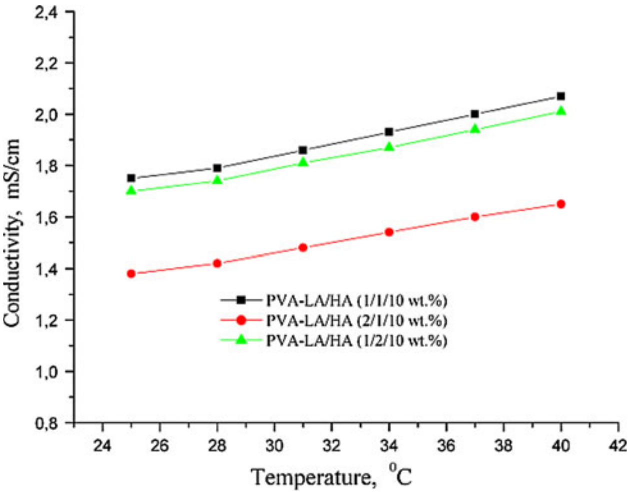

Fig. 14 Conductivity variation with temperature for PVA-co-LA/HA composites

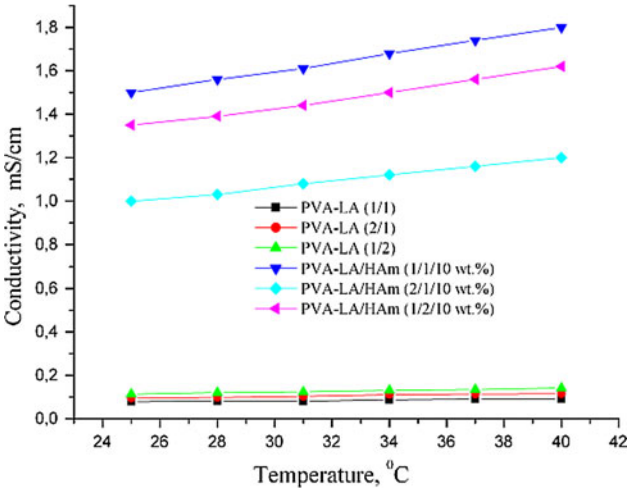

Fig. 15 Conductivity variation with temperature for PVA-co-LA copolymers and PVA-co-LA/HA_m composites

polymeric matrix as well as to improve the homogeneous distribution of the inorganic particles in the polymer matrix, the HA particles were surface-grafted with lactic acid in presence of manganese acetate as catalyst. The grafted modified HA particles were then subjected at a polycondensing in situ procedure with poly(vinyl alcohol). Composite materials PVA-co-LA/HA_m with 140–150 nm hydrodynamic diameters, were obtained. The compatibility of HA_m particles with the polymer matrix is better than in the case of HA, aspect remarked also by the presence of only one Tg value (by DSC), the homogeneity and dispersion of the particles is uniform, no phase separation exist. Concerning the thermal stability of the composite materials achieved with HA_m and HA, it was ascertained that it was influenced by PVA/LA molar ratio in the initial reaction mixture. The thermal stability of the two types of composites lowers with lactic acid percentage raise in copolymer matrix structure, being also influenced by hydroxyapatite type. Generally, the melting temperatures have values comprised between 140 and 190 °C and the glass transition temperatures have lower values than 70 °C, this fact allowing the achievement of some films by hot pressing, films that will be next characterized by mechanical tests, as well as by their biodegradation behavior in controlled laboratory conditions.

Acknowledgments This work was supported by CNCSIS–UEFISCSU, project number 466 PNII—IDEI code_995/2009: Researches in the Field of Polymeric Matrices Design for Sensitive Structures Romania.

References

1. Black J (1992) Biological Performance of Materials: Fundamentals of Biocompatibility. New York, Marcel Dekker
2. Maquet V, Boccaccini AR, Pravata L, Notingher I, Jerome R (2004) Biomaterials 25:4185
3. Kim HW, Song JH, Kim HE (2005) Adv Funct Mater 15:1988
4. Almirall A, Larrecq G, Delgado JAA (2004) Biomaterials 17:3671
5. Geesink RGT, Manley MT (1993) Hydroxyapatite coatings in orthopeadic surgery. Raven Press, New York
6. Frayssinet P, Hardy D, Hanker JS, Giammara BL (1995) Cells Mater 5:125
7. Hu Y, Hu YS, Topolkaraev V, Hiltner A, Baer E (2003) Polymer 44:5681
8. Sheth M, Kumar RA, Dave V, Gross RA, McCarthy SPJ (1997) Appl Polym Sci 66:1495
9. Baiardo M, Frisoni G, Scandola M, Rimelen M, Lips D, Ruffieux K, Wintermantel EJ (2003) Appl Polym Sci 90:731
10. Blumm E, Owen AJ (1995) Polymer 36:4077
11. Tsuji H, Mizuno A, Ikada YJ (1998) Appl Polym Sci 70:2259
12. Yang JM, Chen HL, You JW, Hwang JC (1997) Polym J 29:657
13. Taizo F, Yoshimura M, Tsunoru Y, Yasuo S, Masaki O, Takashi N (2000) Biomaterials 21:889
14. Verheyen CCPM, de Wijn JR, van Blitterswijk CA, de Groot KJ (1992) Biomed Mater Res 26:1277
15. Deng X, Hao J, Wang C (2001) Biomaterials 22:2867
16. Dupraz AMP, de Wijn JR, van der Meer SV, de Groot K (1996) J Biomed Mater Res 30:231
17. Borum-Nicholas L, Wilson O C Jr (2003) Biomaterials 24:3671
18. Liu Q, de Wijn JR, Bakker D, van Blitterswijk CAJ (1996) Mater Sci Mater Med 7:551
19. Liu Q, de Wijn JR, van Toledo M, Bakker D, van Blitterswijk CAJ (1998) Mater Sci Mater Med 9:23
20. Qiu X, Hong Z, Hu J, Chen L, Chen X, Jing X (2005) Biomacromolecules 6:1193
21. Wang X, Li Y, Wei J, de Groot K (2002) Biomaterials 23:4787
22. Liu Q, de Wijn JR, de Groot K, van Blitterswijk CA (1998) Biomaterials 19:1067
23. Dong G-C, Sun J-S, Yao C-H, Jiang George J, Huang C-W, Lin F-H (2001) Biomaterials 22:3179
24. Liu Q, de Wijn JR, van Blitterswijk CAJ (1998) Biomed Mater Res 40:257
25. Kikuchi M, Suetsugu Y, Tanaka J, Akao MJ (1997) Mater Sci Mater Med 8:361
26. Mikos AG, Thorsen AJ, Czerwonka LA, Bao Y, Langer R, Winslow DN, Vacanti JP (1994) Polymer 35:1068

27. Ma PX, Schloo B, Mooney D, Langer RJ (1995) Biomed Mater Res 29:1587
28. Marra K, Campbell P, DiMilla P, Kumta P, Mooney M, Szem J, Weiss L (1999) Mater Res Soc Symp Proc 550:155
29. Marra KG, Szem JW, Kumta PN, DiMilla PA, Weiss LEJ (1999) Biomed Mater Res 47:324
30. Chiellini Emo, Corti Andrea, D'Antone Salvatore, Solaro Roberto (2003) Biodegradation of poly (vinyl alcohol) based materials. Prog Polym Sci 28:963–1014
31. Bolto B, Tran T, Hoang M, Xie Z (2009) Crosslinked poly(vinyl alcohol) membranes. Prog Polym Sci 34:969–981
32. Bajpai AK, Shukla SK, Bhanu S, Kankane S (2008) Responsive polymers in controlled drug delivery. Prog Polym Sci 33: 1088–1118
33. Hong Z, Qiu X, Sun J, Deng M, Chen X, Jing X (2004) Grafting polymerization of L-lactide on the surface of hydroxyapatite nano-crystals. Polymer 45:6699–6706
34. Hong Z, Zhang P, Chaoliang H, Qiu X, Liu A, Chen L, Chen X, Jing X (2005) Nano-composite of poly(L-lactide) and surface grafted hydroxyapatite: Mechanical properties and biocompatibility. Biomaterials 26(32):6296–6304
35. Zou B, Xiaohong L, Zhuang H, Cui W, Zou J, Chen J (2011) Degradation behaviors of electrospun fibrous composites of hydroxyapatite and chemically modified poly(DL-lactide). Polym Degrad Stab 96:114–122
36. Nakajima T, Wang R, Elovaara E, Gonzalez F, Gelboin H, Raunio H, Pelkonen O, Vainio H, Aoyama T (1997) Toluene metabolism by cDNA-expressed human hepatic cytochrome P450. Biochem Pharmacol 53(3):271–277
37. Hanioka H, Hamamura M, Kakino K, Ogata H, Jinno H, Takahashi A, Nishimura T, Ando M (1995) Dog liver microsomal P450 enzyme-mediated toluene biotransformation. Xenobiotica 25(11):1207–1217
38. Qiu X, Hong Z, Junli H, Chen L, Chen X, Jing X (2005) Biomacromolecules 6:1193–1199
39. Hong Zhongkui, Qiu Xueyu, Sun Jingru, Deng Mingxiao, Chen Xuesi, Jing Xiabin (2004) Polymer 45(19):6699–6706
40. Liu Y, Yuan M, Deng X (2003) Eur Polym J 39:977
41. Gong Q, Wang L-Q, Tu K (2006) Carbohydr Polym 64:501
42. Galwey AK, Brown ME (1999) Thermal decomposition of ionic solids. Elsevier, Amsterdam
43. Friedman HLJ (1964) Polym Sci Part C 6:183
44. Friedman HLJ (1966) Polymer Lett 4:323
45. Opfermann J (2000) J Therm Anal Calorim 60:641
46. Kopinke D. F., Muckenzie (1997) J Anal Appl Pyrolysis: 40–41, 43–53
47. Xiao C, Liu H, Gao S, Zhang L (2000) Characterization of poly(vinyl alcohol)-konjac glucomannan blend films. Pure Appl Chem A37(9):1009–1021